

Going beyond the dipole approximation to improve the refinement of magnetic structures by neutron diffraction

M. Rotter* and A. T. Boothroyd

Department of Physics, Clarendon Laboratory, University of Oxford, Parks Road, Oxford OX1 3PU, United Kingdom

(Received 22 December 2008; revised manuscript received 9 March 2009; published 7 April 2009)

We have made an analysis of neutron-diffraction data for a number of rare-earth compounds to assess the use of the dipole approximation in magnetic structure refinements. We present two examples. In the case of CePd₂Si₂, our analysis confirms the published magnetic structure, but we find that use of the “exact” magnetic form factor of Ce³⁺ gives a significantly improved description of the data. For NdBa₂Cu₃O_{6+x}, however, we find that incorrect conclusions have previously been drawn about the magnetic structure through the use of the dipole approximation. We have extended the magnetic modeling suite MCPHASE to enable a straightforward calculation of the higher-order anisotropic terms in the form factor of rare-earth-based systems.

DOI: 10.1103/PhysRevB.79.140405

PACS number(s): 75.25.+z, 61.05.fd, 75.20.Hr, 75.50.Ee

Neutron diffraction is the standard method for determining magnetic structures. Magnetic neutron diffraction arises from the interaction between the magnetic moment of the neutron and magnetic fields in the sample associated with orbital currents and intrinsic spin of unpaired electrons. The distribution of scattered neutrons is modulated by a form factor, which for elastic scattering is the Fourier transform of the magnetization. Most state-of-the-art magnetic structure refinement procedures employ the *dipole approximation* for the form factor, which assumes that the spatial distribution of magnetization in an atom or ion is isotropic. This approximation is strictly valid only in the limit of small scattering vectors, although for many problems it is accurate enough to enable the magnetic structure to be solved. However, with the best neutron-diffraction instrumentation it is possible to measure diffraction intensities with sufficient precision that the dipole approximation is not always satisfactory. For example, in recent studies on Ce-based compounds it has been shown that the modeling of diffraction data can be improved by including higher-order corrections to the dipole approximation.¹⁻³

The purpose of this Rapid Communication is twofold. First, we wish to demonstrate the importance of going beyond the dipole approximation in the analysis of magnetic neutron-diffraction data. The focus here is on rare-earth ions, but corrections to the dipole approximation are expected to be even larger for transition metals.^{4,5} Second, we report the incorporation of the exact form factor into the MCPHASE modeling suite⁶⁻¹⁰ so that rare-earth magnetic structure calculations similar to those presented here can be performed for other compounds.

In the standard formalism¹¹ the elastic magnetic neutron-scattering cross section $(d\sigma/d\Omega)_{\text{mag}}$ is proportional to the square of the magnetic structure factor F_M ,

$$\left(\frac{d\sigma}{d\Omega}\right)_{\text{mag}} \sim |F_M|^2, \quad (1)$$

where

$$F_M = \sum_d \langle \hat{\mathbf{M}}_{\perp d}(\mathbf{Q}) \rangle \exp(i\mathbf{Q} \cdot \mathbf{R}_d) \exp(-W_d) \quad (2)$$

and

$$\langle \hat{\mathbf{M}}_{\perp d}(\mathbf{Q}) \rangle = \mathbf{Q} \times \{ \langle \hat{\mathbf{M}}_d(\mathbf{Q}) \rangle \times \mathbf{Q} \} / Q^2. \quad (3)$$

The summation is over the ions indexed by d in the magnetic unit cell, with displacements \mathbf{R}_d from the origin. The scattering vector is denoted by \mathbf{Q} , with $Q=|\mathbf{Q}|$, $\hat{\mathbf{M}}_d(\mathbf{Q})$ is the Fourier transform of the magnetization operator and $\exp(-W_d)$ is the Debye-Waller factor.

In the dipole approximation, $\langle \hat{\mathbf{M}}_d(\mathbf{Q}) \rangle$ may be separated into a product of a magnetic form factor $f_{\text{dip}}(\mathbf{Q})$, which is a scalar function of Q , and the thermal expectation value of the magnetic moment $\langle \hat{\mathbf{m}}_d \rangle$ of the ion,

$$\langle \hat{\mathbf{M}}_d(\mathbf{Q}) \rangle = f_{\text{dip}}(\mathbf{Q}) \langle \hat{\mathbf{m}}_d \rangle. \quad (4)$$

For rare-earth ions the dipole form factor is given by

$$f_{\text{dip}}(\mathbf{Q}) = \langle j_0(\mathbf{Q}) \rangle + \frac{2-g_J}{g_J} \langle j_2(\mathbf{Q}) \rangle, \quad (5)$$

where g_J denotes the Landé factor of the rare-earth ion. Analytical approximations for the expectation values of the spherical Bessel functions $\langle j_l(\mathbf{Q}) \rangle$ (for $l=0,2,4,6$) are available for many ions and have been tabulated.¹² Many standard refinement codes for magnetic structures make use of these tables and compute the magnetic form factor by the dipole approximation.

In order to go beyond the dipole approximation one must include higher-order multipoles in the expansion of the spin density and orbital current density. This was attempted by Trammell,¹³ and the theory was presented in a more compact form using Racah tensors by Johnston,¹⁴ and others.¹⁵ The resulting form factor is anisotropic and includes the expectation values $\langle j_4(\mathbf{Q}) \rangle$ and $\langle j_6(\mathbf{Q}) \rangle$ in addition to $\langle j_0(\mathbf{Q}) \rangle$ and $\langle j_2(\mathbf{Q}) \rangle$.

The calculation of the form factor requires diagonalization of the appropriate Hamiltonian, which typically includes the crystalline electric field, magnetic interactions and any external field present, and calculation of the matrix elements of $\hat{\mathbf{M}}(\mathbf{Q})$ (we omit the index d in what follows for brevity). A natural basis for the rare-earth ions is the atomic wave functions $|SLJM\rangle$, where $M=-J, -J+1, \dots, J$. The formulae for the matrix elements are rather intimidating, but Lovesey¹¹ presented them in a compact form which we reproduce

below.¹⁶ To be consistent with Ref. 11 we write the matrix elements in terms of the scattering operator $\hat{Q}_\alpha \equiv -\hat{M}_\alpha(Q)/(2\mu_B)$ (with $\alpha=x,y,z$ and μ_B the Bohr magneton) as follows:

$$\begin{aligned} \langle SLJM|\hat{Q}_x|SLJM'\rangle &= \frac{\sqrt{4\pi}}{2} \sum_{K',Q'} \frac{Z(K')}{K'} P(K',Q') [Y_{K'-1,Q'+1}(\tilde{\mathbf{Q}})\sqrt{(K'-Q')(K'-Q'-1)} \\ &\quad - Y_{K'-1,Q'-1}(\tilde{\mathbf{Q}})\sqrt{(K'+Q')(K'+Q'-1)}], \end{aligned} \quad (6)$$

$$\begin{aligned} \langle SLJM|\hat{Q}_y|SLJM'\rangle &= \frac{-i\sqrt{4\pi}}{2} \sum_{K',Q'} \frac{Z(K')}{K'} P(K',Q') [Y_{K'-1,Q'+1}(\tilde{\mathbf{Q}})\sqrt{(K'-Q')(K'-Q'-1)} \\ &\quad + Y_{K'-1,Q'-1}(\tilde{\mathbf{Q}})\sqrt{(K'+Q')(K'+Q'-1)}], \end{aligned} \quad (7)$$

$$\langle SLJM|\hat{Q}_z|SLJM'\rangle = \sqrt{4\pi} \sum_{K',Q'} \frac{Z(K')}{K'} P(K',Q') Y_{K'-1,Q'}(\tilde{\mathbf{Q}})\sqrt{(K'-Q')(K'+Q')}, \quad (8)$$

where

$$Z(K') = c_{K'-1}\langle j_{K'-1}(Q)\rangle + c_{K'+1}\langle j_{K'+1}(Q)\rangle \quad (9)$$

$$P(K',Q') = (-1)^{J-M'} \frac{\begin{pmatrix} K' & J & J \\ -Q' & M' & -M \end{pmatrix}}{\begin{pmatrix} K' & J & J \\ 0 & J & -J \end{pmatrix}}. \quad (10)$$

The coefficients $c_{K'}$ ($K'=1,3,5,7$) have been tabulated for the different rare-earth ions (see Table 11.1 of Ref. 11). The $Y_{l,m}(\tilde{\mathbf{Q}})$ are spherical harmonics evaluated for the direction of the scattering vector. The factor $P(K',Q')$ is defined in terms of $3j$ symbols, which restrict $Q'=M'-M$.

As a first example of this approach we will analyze magnetic diffraction data of the heavy fermion superconductor CePd₂Si₂ (Néel temperature $T_N \sim 10$ K).¹⁷ To go beyond the dipole approximation we need the eigenstates of each magnetic ion. The most straightforward method to obtain these is to fit a mean field on each site in the magnetic unit cell so as to stabilize the observed magnetic structure. Using an adequate parametrization of the crystal field and these mean fields one can calculate the eigenstates in the $|SLJM\rangle$ basis and hence compute the scattering cross section from Eqs. (1)–(10). However, more insight can be obtained if the mean fields are calculated directly from a model based on the fundamental magnetic interactions. We follow this second approach for CePd₂Si₂.

The formalism is based on the following Hamiltonian \mathcal{H} for rare-earth systems:

$$\mathcal{H} = \sum_{s,l,m} B_l^m O_l^m(\mathbf{J}^s) - \frac{1}{2} \sum_{ss'} \mathcal{J}_{\alpha\beta}(ss') \mathbf{J}_\alpha^s \mathbf{J}_\beta^{s'}. \quad (11)$$

$\alpha, \beta = x, y, z$

The first term describes the crystal field acting on the ion at site s in terms of Stevens operators O_l^m , and the second term is the magnetic two-ion interaction. The crystal-field parameters B_l^m and exchange interactions $\mathcal{J}(ss')$ were taken from Refs. 18 and 19. In addition to the isotropic exchange interaction $\mathcal{J}_{\alpha\beta}(ss') = \mathcal{J}(ss')\delta_{\alpha\beta}$ (here $\delta_{\alpha\beta}$ is the Kronecker symbol), some sort of anisotropy is needed in order to stabilize

the (experimentally observed) longitudinal modulation of the antiferromagnetic spin density wave with respect to a transversal one. It turns out that the classical dipole (CD) anisotropy,

$$\mathcal{J}_{\alpha\beta}^{\text{CD}}(ss') = (g_J\mu_B)^2 \frac{3(R_s^\alpha - R_{s'}^\alpha)(R_s^\beta - R_{s'}^\beta) - \delta_{\alpha\beta}|\mathbf{R}_s - \mathbf{R}_{s'}|^2}{|\mathbf{R}_s - \mathbf{R}_{s'}|^5}, \quad (12)$$

would stabilize a transversal modulation. However, a classical dipole interaction (12) with reversed sign, i.e.,

$$\mathcal{J}_{\alpha\beta}(ss') = \mathcal{J}(ss')\delta_{\alpha\beta} - \mathcal{J}_{\alpha\beta}^{\text{CD}}(ss'), \quad (13)$$

succeeds in reproducing the reported longitudinally modulated magnetic structure. Note that this procedure, though handy for our purpose, does not provide an explanation of the origin of the anisotropy in this system. Based on this model we found a mean field of ± 16.7 T on the two Ce sites of the antiferromagnetic unit cell.

Using this mean field in combination with the crystal field we obtained the single-ion eigenvalues and eigenstates and hence evaluated the magnetic neutron-diffraction intensity via Eqs. (1)–(10). Figure 1 compares the magnetic Bragg-peak intensities calculated this way with those obtained via the dipole approximation. Deviations between the two methods are large (typically 20%–50%) at higher scattering vectors. Using the exact form factor we obtain a significant improvement in the description of the experimental intensities. The improvement is reflected in the standard goodness-of-fit parameters R_p (Ref. 20) and χ^2 .²¹ The dipole approximation gives $R_p = 15.6$ and $\chi^2 = 27.2$, whereas going beyond the dipole approximation we obtain $R_p = 8.4$ and $\chi^2 = 7.7$. Note that magnetic intensities were scaled by a common factor in order to obtain a reasonable fit. This shows that the moment calculated on the basis of our model Hamiltonian comes out about 40% too large. In an alternative approach we took the mean field as a fitting parameter and obtained a smaller value for the mean field (corresponding to a smaller magnetic moment). This approach results in a slightly higher R_p factor but will not substantially alter the conclusions.

The case of CePd₂Si₂ shows that going beyond the dipole approximation significantly improves the description of ex-

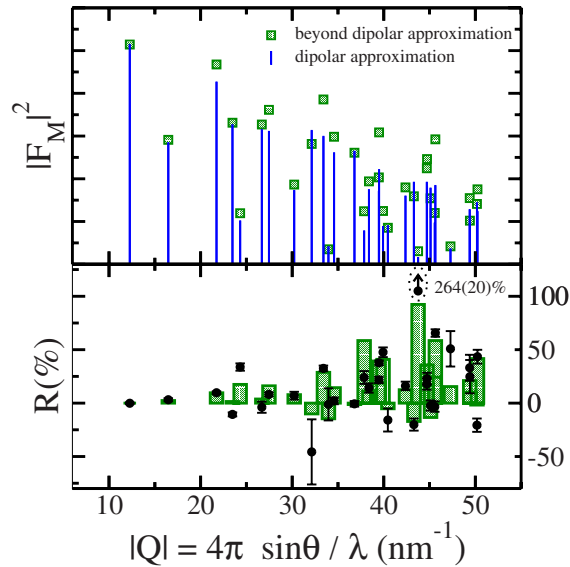


FIG. 1. (Color online) Magnetic Bragg-peak intensities for CePd_2Si_2 calculated (i) in the dipole approximation and (ii) going beyond the dipole approximation (upper figure). In both cases the moments were assumed to be aligned parallel to the $[110]$ direction. The lower figure shows deviations between the exact calculation and dipole approximation expressed as $R = 100(|F_M^{\text{exact}}|^2 - |F_M^{\text{dip}}|^2) / |F_M^{\text{dip}}|^2$ (bars) and comparison with experimental data obtained on a single crystal at $T = 1.3$ K (Ref. 17) plotted as $R = 100(|F_M^{\text{exp}}|^2 - |F_M^{\text{dip}}|^2) / |F_M^{\text{dip}}|^2$ (symbols).

perimental magnetic neutron-diffraction intensities. In the next example we will demonstrate that use of the dipole approximation may even lead to incorrect conclusions about the magnetic structure.

In Ref. 22 a neutron-diffraction study of magnetic ordering in $\text{NdBa}_2\text{Cu}_3\text{O}_{6+x}$ was reported. Diffraction data were collected from the single-crystal samples and the intensities fitted to magnetic structure models in which the dipole form factor was used. For a crystal of superconducting $\text{NdBa}_2\text{Cu}_3\text{O}_{6.97}$ the best description of the experimental data was obtained with a model for the antiferromagnetic structure in which the moments point not along the c axis but tilted by $\sim 12^\circ$ from the c axis (see Fig. 2).

Although puzzling, a tilted moment which breaks the

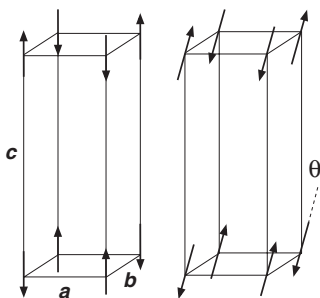


FIG. 2. Models for the magnetic structure of $\text{NdBa}_2\text{Cu}_3\text{O}_{6.97}$. Only the Nd moments are shown. A magnetic structure refinement with the dipole form factor suggests a tilt of the spin axis from the c direction of $\theta = 12^\circ$ (right). With the exact anisotropic form factor a better fit is achieved with moments parallel to c (left).

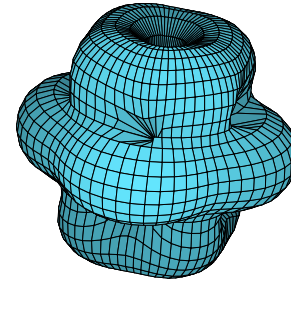


FIG. 3. (Color online) $4f$ charge density of Nd^{3+} calculated from the action of the crystal field in $\text{NdBa}_2\text{Cu}_3\text{O}_{6.97}$ at $T = 2$ K.

crystal symmetry is not totally implausible. For example, an earlier study of the magnetic order in $\text{PrBa}_2\text{Cu}_3\text{O}_{6+x}$ (Ref. 23) had revealed just such a tilt which originated from a pseudodipolar Pr-Cu interaction coupling the magnetic ordering on the Pr and Cu sublattices. However, superconducting $\text{NdBa}_2\text{Cu}_3\text{O}_{6.97}$ has no Cu magnetic order so the apparent tilting of the Nd moments was a surprise.

Here we repeat the magnetic structure refinement using the same data but calculating the diffraction intensities with the anisotropic form factor of Nd^{3+} . The ground state of the Nd^{3+} ion was determined by fitting crystal-field spectra^{24–26} and susceptibility data^{27,28} simultaneously using a full intermediate coupling calculation including mixing of all levels up to 2 eV.²⁹ Crystal-field parameters derived for $\text{PrBa}_2\text{Cu}_3\text{O}_{6+x}$ (Ref. 30) scaled to Nd^{3+} were taken as starting values for the fit. Only data for tetragonal (nonsuperconducting) $\text{NdBa}_2\text{Cu}_3\text{O}_{6+x}$ were included in this analysis. The best-fit parameters from this analysis were converted into the coefficients of the Stevens operators required in Eq. (11). The values so obtained are $B_2^0 = -236.9 \mu\text{eV}$, $B_4^0 = +16.76 \mu\text{eV}$, $B_4^4 = -32.606 \mu\text{eV}$, $B_6^0 = -0.237 \mu\text{eV}$, and $B_6^4 = -6.324 \mu\text{eV}$. The neglect of the four additional orthorhombic crystal-field parameters (B_2^2 , B_4^2 , B_6^2 , and B_6^6) required to describe completely the crystal field in orthorhombic $\text{NdBa}_2\text{Cu}_3\text{O}_{6.97}$ has only very small influence on the shape of the $4f$ magnetization density. This was checked by repeating the form factor calculations with estimated orthorhombic crystal-field parameters derived from those of $\text{PrBa}_2\text{Cu}_3\text{O}_{6+x}$ by scaling.

Figure 3 shows the anisotropic charge density at $T = 2$ K resulting from the crystal-field interaction alone. In order to stabilize magnetic order it is necessary to introduce an antiferromagnetic interaction between the two sublattices. For our calculation we used $\mathcal{J}(ss') = -5 \mu\text{eV}$ corresponding to a mean field of 1.8 T on each Nd^{3+} ion (at $T = 0.3$ K). This interaction, together with the crystal field, leads to a magnetic structure with moments parallel to c for all temperatures $T < T_N = 0.62$ K. In order to simulate the canted magnetic structure shown in Fig. 2 we introduced in addition to $\mathcal{J}(ss')$ a biquadratic interaction $-1/2 \sum_{ss'} K(ss') (\mathbf{J}_s \cdot \mathbf{J}_{s'})^2$ with $K(ss') = 11 \mu\text{eV}$.

In Table I we list the measured magnetic neutron-diffraction intensities for $\text{NdBa}_2\text{Cu}_3\text{O}_{6.97}$ together with the fitted intensities calculated first by the dipole approximation and second with the full anisotropic form factor. In the calculation with the dipole form factor the best fit is achieved with the Nd^{3+} moment tilted 12° away from the c axis, as

TABLE I. Observed and calculated integrated intensities of the magnetic reflections from the Nd magnetic structure of NdBa₂Cu₃O_{6.97} at 0.3 K. θ is the angle of the Nd moments from the c axis. The magnetic intensities are calculated with the dipole form factor and with the “exact” anisotropic form factor. For $\theta = 12^\circ$ contributions from equivalent magnetic domains have been averaged.

h	k	l	$ Q $ (1/Å)	$I_{\text{obs}} \pm \sigma_{\text{obs}}$ Ref. 22	$I_{\text{mag}}^{\text{dip}}$ $\theta=0$	$I_{\text{mag}}^{\text{dip}}$ $\theta=12^\circ$	I_{mag} $\theta=0$	I_{mag} $\theta=12^\circ$
0.5	0.5	0.5	1.1749	115 ± 4	117	110	111	104
0.5	0.5	1.5	1.3981	84 ± 3	81	78	78	75
0.5	0.5	2.5	1.7617	50 ± 1	49	49	49	49
0.5	0.5	3.5	2.1969	29 ± 1	30	32	32	33
0.5	0.5	4.5	2.6690	22 ± 2	19	21	21	23
0.5	0.5	5.5	3.1616	15 ± 1	12	15	15	17
0.5	0.5	6.5	3.6663	12 ± 1	8	11	10	13
1.5	1.5	0.5	3.4424	77 ± 8	87	82	78	74
1.5	1.5	1.5	3.5248	65 ± 7	82	77	74	70
1.5	1.5	2.5	3.6842	59 ± 5	73	68	68	64
1.5	1.5	3.5	3.9110	51 ± 5	60	58	60	57
χ^2					4.16	2.07	2.07	3.67
R_p					11.4	8.48	7.69	8.37

found in Ref. 22. However, when the anisotropic form factor is employed the best-fit model has the moments parallel to the c axis. Indeed, the R_p value for this fit is lower than that for the published magnetic structure (with a tilted moment). We conclude, therefore, that the most probable direction of the ordered Nd³⁺ moment is along the c axis. Apart from solving a longstanding puzzle, this exercise has illustrated how the use of the dipole approximation for calculating magnetic scattering can in some cases lead to an incorrect magnetic structure refinement.

We have performed similar calculations for a series of other rare-earth-based antiferromagnets including CePd₂Ge₂ and HoF₃ and compared these to available experimental data. The results indicate that the modeling of experimental mag-

netic neutron-diffraction data can be improved significantly by employing the anisotropic multipolar magnetic form factor. Moreover, as we found here in the case of NdBa₂Cu₃O_{6.97}, using the dipole approximation may lead to an incorrect magnetic structure. Thus, we are convinced that state-of-the-art magnetic structure analysis should go beyond the dipole approximation. In order to make such refinements accessible to a wider scientific community we have adapted the magnetic modeling suite MCPHASE (Ref. 6) to incorporate the anisotropic form factor.

We thank B. Fåk and E. Ressouche for helpful discussions and for providing us with the single-crystal data of CePd₂Si₂. This work was supported by the Engineering and Physical Sciences Research Council of Great Britain.

*[http://www.physics.ox.ac.uk/users/rotter;](http://www.physics.ox.ac.uk/users/rotter;martin.rotter@physics.ox.ac.uk)
martin.rotter@physics.ox.ac.uk

¹F. Givord *et al.*, J. Phys.: Condens. Matter **16**, 1211 (2004).

²K. Kuwahara *et al.*, J. Phys. Soc. Jpn. **76**, 093702 (2007).

³J. Schweizer *et al.*, J. Phys.: Condens. Matter **20**, 135204 (2008).

⁴S. Shamoto *et al.*, Phys. Rev. B **48**, 13817 (1993).

⁵A. Longmore *et al.*, Phys. Rev. B **53**, 9382 (1996).

⁶M. Rotter *et al.*, MCPHASE, a software package for the calculation of phase diagrams and magnetic properties of rare-earth systems (2002–2008), available at <http://www.mcphase.de>

⁷M. Rotter, J. Magn. Magn. Mater. **272-276**, e481 (2004).

⁸M. Rotter *et al.*, Physica B **345**, 231 (2004).

⁹M. Rotter, Comput. Mater. Sci. **38**, 400 (2006).

¹⁰J. Jensen and M. Rotter, Phys. Rev. B **77**, 134408 (2008).

¹¹S. W. Lovesey, *Theory of Neutron Scattering from Condensed Matter* (Clarendon, Oxford, 1984).

¹²*The International Tables for X-ray Crystallography*, edited by T. Hahn (D. Reidel, Dordrecht, Holland, 1983), Vol. A.

¹³G. T. Trammell, Phys. Rev. **92**, 1387 (1953).

¹⁴D. F. Johnston, Proc. Phys. Soc. London **88**, 37 (1966).

¹⁵S. W. Lovesey, J. Phys. C **2**, 470 (1969); D. F. Johnston and D.

E. Rimmer, *ibid.* **2**, 1151 (1969); E. Balcar and S. W. Lovesey, *Theory of Magnetic Neutron and Photon Scattering*, (Clarendon, Oxford, 1989); C. Stassis and H. W. Deckman, Phys. Rev. B **12**, 1885 (1975).

¹⁶Note that in Ref. 11 there is a small error in equations (11.141) and (11.142): the imaginary i has been misplaced.

¹⁷N. Kernavanois *et al.*, Phys. Rev. B **71**, 064404 (2005).

¹⁸N. H. van Dijk *et al.*, Phys. Rev. B **61**, 8922 (2000).

¹⁹P. Hansmann *et al.*, Phys. Rev. Lett. **100**, 066405 (2008).

²⁰ $R_p = 100 \sum_{hkl} |I_{\text{calc}}(hkl) - I_{\text{obs}}(hkl)| / \sum_{hkl} |I_{\text{obs}}(hkl)|$

²¹ $\chi^2 = \sum_{hkl=1}^N [I_{\text{calc}}(hkl) - I_{\text{obs}}(hkl)]^2 / N \sigma_{\text{obs}}^2(hkl)$

²²A. T. Boothroyd *et al.*, Phys. Rev. B **60**, 1400 (1999).

²³A. T. Boothroyd *et al.*, Phys. Rev. Lett. **78**, 130 (1997).

²⁴P. Allenspach *et al.*, Z. Phys. B: Condens. Matter **95**, 301 (1994).

²⁵L. Soderholm *et al.*, Phys. Rev. B **43**, 7923 (1991).

²⁶H. Dröbler *et al.*, Z. Phys. B: Condens. Matter **100**, 1 (1996).

²⁷N. Senthilkumaran *et al.*, Physica B **223-224**, 565 (1996).

²⁸V. Nekvasil *et al.*, J. Magn. Magn. Mater. **226-230**, 985 (2001).

²⁹A. T. Boothroyd, SPECTRE, a program to calculate the spectra of f electrons in crystal fields in the intermediate coupling approximation (1989–2008).

³⁰A. T. Boothroyd *et al.*, Physica C **217**, 425 (1993).